Materials and Structures (2020) 53:56
https://doi.org/10.1617/s11527-020-01488-7

ORIGINAL ARTICLE

Fatigue fracture of fibre reinforced concrete in flexure

Stefie J. Stephen · Ravindra Gettu

Received: 28 July 2019 / Accepted: 1 May 2020 / Published online: 13 May 2020

Abstract An experimental study on the behaviour of fibre reinforced concrete under flexure is presented, where pre-cracked notched beams were tested under cyclic loading for concrete with different dosages of hooked-ended steel fibres. The fatigue crack growth and stiffness degradation during the cycles are discussed in term of the rate of evolution of crack opening, and the critical crack opening is identified, beyond which the crack growth becomes unstable. *S*–*N* curves have been proposed with respect to the critical crack opening as these would be more relevant to design avoiding sudden failure. It is evident that higher dosages of fibres improve the fatigue life of cracked concrete only when the magnitudes of the cyclic loading are high, and that the effect of dosage is insignificant at lower magnitudes. For the fibre concretes considered here, the endurance limit seems to be about 50% of the pre-crack load in the post-peak regime.

Keywords Fatigue fracture · Fibre reinforced concrete · Notched beam testing · *S*–*N* curves · Fatigue damage · Stiffness degradation · Critical crack opening

1 Introduction

Fatigue is a process of progressive detrimental changes occurring in a structure subjected to repeated cyclic loading. Most fibre reinforced concrete (FRC) structures are subjected to cyclic loads, in the form of traffic movement, wind and wave action, thermal variations, machine vibration etc. Some structures could experience millions of stress cycles during their service lives, which eventually reduce the material performance in terms of strength, stiffness and toughness [1] due to cracking or damage accumulation. Fatigue could also pose problems in terms of aggravating crack widths and deflections during the service life, even if failure does not occur [2].

The fatigue fracture process in the matrix or plain concrete [3] begins with crack initiation, which depends on characteristics such as the bulk tensile strength, porosity and matrix-aggregate interface properties [4]. This is followed by slow crack progression up to a critical size, subsequent to which the crack propagates rapidly and coalesces with microcracks, leading to failure. However, in FRC

Electronic supplementary material The online version of this article (https://doi.org/10.1617/s11527-020-01488-7) contains supplementary material, which is available to authorized users.

S. J. Stephen (✉) · R. Gettu
Department of Civil Engineering, IIT Madras, Chennai 600036, India
e-mail: stefie.j.s@gmail.com

R. Gettu
e-mail: gettu@iitm.ac.in

under cyclic tensile loading, various researchers have observed that the fibre-matrix interface plays a major role in improving the fatigue life by dissipating energy and facilitating stress transfer across the crack faces, which shields the crack-tip [5–8]. On the flexural fatigue of FRC, extensive research has been carried out in the pre-peak regime (i.e., before or just after crack initiation), based on tests of unnotched [9] or notched beams [2], and fatigue models have been developed [10] to understand the failure response [11–13]. Such work has shown that fibres are useful in resisting higher fatigue stresses, where further crack growth and widening is inhibited by fibre bridging and pull-out [14], with the fatigue life generally increasing with higher fibre aspect ratio and dosage [15, 16]. Nevertheless, it was also seen that the cyclic loading progressively degrades the fibre-matrix interface [17] and leads to the reduction of residual strength of the concrete [18]. The fatigue performance of concrete reinforced with steel fibres has been shown to be superior to that reinforced with polymer or glass fibres. This is attributed to the higher stiffness of the steel fibre, which helps in improving crack bridging; among steel fibres, the hooked-ended ones yield higher endurance limits compared to those with straight or corrugated steel fibres due to better anchorage [19, 20]. Stiffness degradation, reflecting progressive crack growth, is found to be a major consequence of cyclic loading, in both plain and fibre reinforced concrete [2]. A recently-published paper of Carlesso et al. [21] presents an extensive review of fatigue studies on FRC that can be referred to for further details.

The bridging of the crack by the fibres is most effective after the formation of the fracture process zone (FPZ), and consequently it would be appropriate to assess the fatigue performance of FRC in the post-peak regime [22, 23]. More importantly, considering that FRC structures are designed based on the post-cracking toughness parameters [12, 24, 25], the need for more fatigue studies on cracked concrete has become imperative. Granju et al. [26] performed post-peak fatigue tests on concrete with different types of steel fibres at a dosage of 65 kg/m^3. They applied cyclic loading at different stress ratios (with the maximum load in each cycle being 80, 60 or 50% of the load-carrying capacity, and the minimum load being 10%), after attaining a crack opening of 0.3 mm through monotonic loading. They found that 60 mm long hooked-ended steel fibres yielded better performance, exhibiting an endurance limit of 50% of the load-carrying capacity and surviving fatigue when the load is cycled below this limit. Recently, Germano et al. [23] performed fatigue tests on cracked concrete with similar but shorter fibres (i.e., 35 mm length), at two dosages. In their tests, cyclic loading was applied when the load dropped to 95% of the peak load under monotonic loading, with the maximum load in the cycles being 85, 75 or 65% of the load-carrying capacity and a constant amplitude of 50% of the load-carrying capacity. They found failure to occur when the applied load reaches the envelope load-crack opening curve (obtained from monotonic loading). They also concluded that the incorporation of fibres is evidently beneficial in increasing the fatigue life when the maximum load during the cycles is high. They proposed that the use of higher dosages (e.g., 1% volume fraction of steel fibres) may not necessarily lead to better fatigue response and suggested that the 0.5% volume fraction could be the optimum. The more recent work of Carlesso et al. [21] investigated the degree of damage at different fatigue loading levels on cracked FRC, considering a 100 MPa concrete with 150 kg/m^3 of 13 mm long straight steel fibres, having a diameter of 0.16 mm. They found failure to occur mainly due to the pullout of the fibres from the matrix, especially since the fibres used were smooth and with no mechanical anchorage. All these works emphasize the need for more studies to improve the understanding of the fatigue performance of cracked FRC.

Typically, fatigue testing is conducted under load control with specified lower and upper fatigue stress limits, under constant amplitude non-reversed sinusoidal loads, with a frequency varying between 2 and 20 Hz. It is seen from the literature that the loading frequency does not have any significant influence in the range of 1 to 7 Hz, although very low frequencies are generally associated with slightly lower fatigue strengths and larger permanent deformation [27, 28]. Further, the frequency of traffic movement in typical urban roads ranges from 3 to 16 Hz [29]. Hence, in this work, the fatigue loading is applied at a frequency of 5 Hz.

Here, the fatigue performance in the post-peak regime is evaluated for concrete with different dosages of hooked-ended steel fibres (typically used in applications such as slabs-on-grade and pavements), using notched beams tested under three-point loading. The

S–N or Wöhler diagrams are plotted, based on which fatigue models are proposed for these concretes. The level of fatigue damage is described in terms of crack opening and stiffness degradation with the loading–unloading cycles. The fatigue testing procedure is similar to that of Granju et al. [26], except that pre-cracking is done until a crack width or crack mouth opening displacement (CMOD) of 0.5 mm instead of 0.3 mm, so that the fatigue response can be related to $f_{R,1}$ (as in EN 14651:2005 [30]), which is the residual strength at the CMOD of 0.5 mm, a main design parameter for most FRC structures in the service limit state (SLS). The critical crack opening at which the fatigue crack growth becomes unstable is identified, and an *S–N* model based on the number of cycles to reach the critical crack opening is proposed to avoid sudden failure associated with the end of fatigue life.

2 Experimental programme

The present study is based on fracture tests of concrete with a 28-day characteristic cube strength of 40 MPa (having proportions of cement: sand: coarse aggregate: water as 1:2:3:0.45, and incorporating portland pozzolana cement and aggregates with maximum size of 20 mm). Fibres described in Table 1 have been incorporated in the concrete, and the toughness parameters of the FRCs, determined as per EN 14651:2005 [30] from tests at a constant CMOD rate of 1 μm/s at the age of 28 days, are listed in Table 2 (see [31] for more details). Six batches of concrete were made for each type of concrete, and 5 beams were cast from each batch. For every fatigue loading level, 6 beams of each concrete were tested at the age of 3 months, drawing one from each batch; overall, data from 120 tests were used in the fatigue analysis. The test configuration conforms to EN 14651:2005 [30], with the dimensions of the specimen being 150 × 150 × 700 mm, with a span of 500 mm; the load is applied perpendicular to the direction of casting and a notch of 25 mm depth is cut at the mid-span. The CMOD is measured using a clip gauge mounted on knife edges placed across the notch faces.

Table 1 Details of the fibres and their dosages

Parameter	Steel fibres
Fibre description	Cold-drawn, hooked-ended
Specific gravity (g/cc)	7.8*
Tensile strength (MPa)	1225*
Length (mm)	60
Diameter (mm)	0.75
Dosages	0, 10, 30, 45 kg/m^3

*Values provided by the manufacturer

The tests have been performed in a 1 MN dynamic servohydraulic system with closed-loop control and computer-based data acquisition; a 100 kN load cell was used for monitoring the applied load. The beam is first loaded monotonically under CMOD control, at a rate of 1 μm/sec, until the CMOD reaches 0.5 mm. At this point, corresponding to the residual load $F_{R,1}$ at the CMOD of 0.5 mm, the beam is unloaded. Subsequently, cyclic loading is applied under load control, at a frequency of 5 Hz, between the upper fatigue load, F_u (varied as 90, 80, 70, 60 and 50% of $F_{R,1}$), and lower fatigue load, F_l (set at 10% of $F_{R,1}$), on the cracked beams. The fatigue test is performed until 2 million cycles of loading, the specimen breaks or the CMOD reaches 5 mm, whichever occurs first. Specimens that survive 2 million cycles (i.e., run-out specimens) are subsequently loaded monotonically to determine the residual post-fatigue response (as illustrated in Fig. 1). The load and CMOD are recorded every 100 cycles, except for the last 100 cycles during which the data is logged continuously. The beam notation is based on the compressive strength of the concrete, type of fibres, fibre dosage in kg/m^3 and the maximum fatigue loading level expressed as percentage of $F_{R,1}$; e.g., M40SF45_90% denotes 40 MPa grade concrete with steel fibres (SF) at 45 kg/m^3, subjected to a maximum fatigue load corresponding to 90% of $F_{R,1}$.

3 Test results

Typical load-CMOD curves for the M40SF45 beams obtained during pre-cracking and cyclic loading with 90% and 50% of $F_{R,1}$ are shown in Fig. 2, along with the monotonic flexural response (at 28 days) obtained from companion specimens (shown as a grey band representing the highest and lowest values at different CMOD values in 6 specimens). The load-CMOD response for the last 100 cycles, where most of the fatigue damage occurs, is shown on the graphs for

Table 2 Toughness parameters of the FRCs studied here

Dosage of fibre in concrete (kg/m^3)	LOP (MPa)	Residual flexural strengths at different CMODs			
		0.5 mm $f_{R,1}$ (MPa)	1.5 mm $f_{R,2}$ (MPa)	2.5 mm $f_{R,3}$ (MPa)	3.5 mm $f_{R,4}$ (MPa)
0	5.61 ± 0.10	0.69 ± 0.21	–	–	–
10	5.15 ± 0.40	2.05 ± 0.27	1.89 ± 0.31	1.90 ± 0.26	1.76 ± 0.36
30	5.52 ± 0.47	4.09 ± 0.59	4.86 ± 0.83	5.04 ± 0.91	4.92 ± 0.94
45	6.21 ± 0.47	6.11 ± 0.33	6.85 ± 0.08	6.82 ± 0.29	6.41 ± 0.33

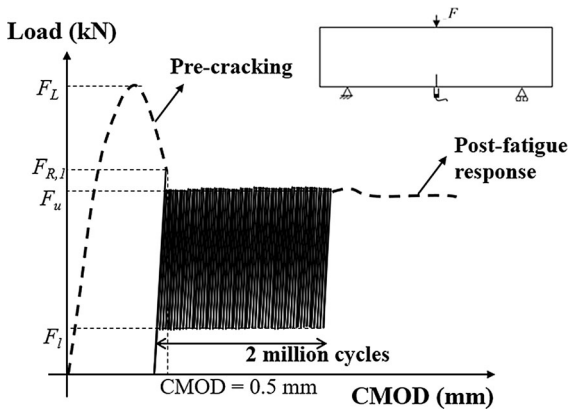

Fig. 1 Illustration of the test procedure

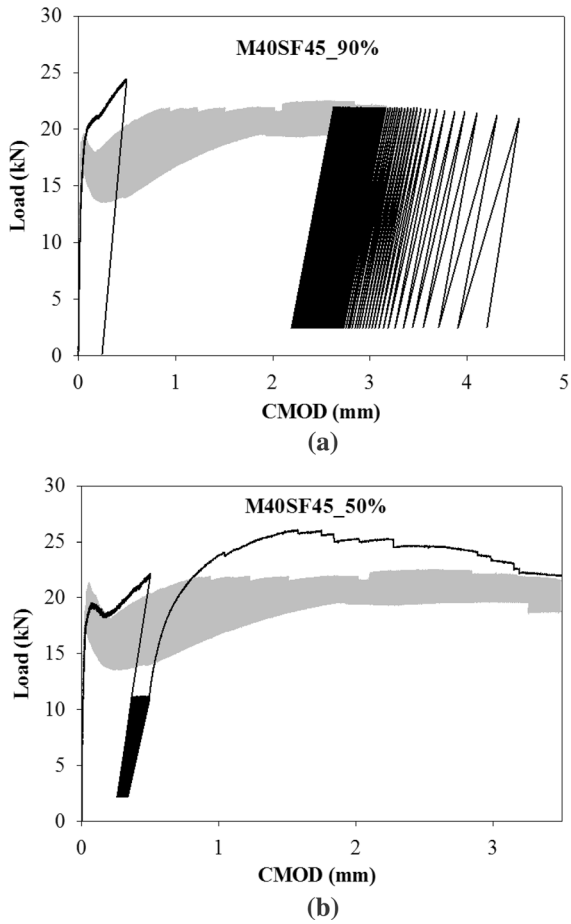

Fig. 2 Typical load versus CMOD curves for M40SF45 concrete beams under maximum fatigue load equal to **a** 90% and **b** 50% of $F_{R,1}$

specimens that failed under cyclic loading (e.g., Fig. 2a). Typical data for all the different fibre dosages and load levels tested can be seen in the Supplementary Material. It is evident that the CMOD increases gently with the cycles until just before failure. Consequently, the variation in the load-CMOD slope during loading–unloading is only significant during the final cycles. This suggests that fatigue damage, indicated by the decrease in slope (as also observed by González et al. [18]), occurs rapidly when the loads are close to the envelope of the monotonic curve whereas for lower loads the crack propagation is slower with failure occurring only after large crack widths. The rapid increase in CMOD occurs after relatively greater number of cycles when the fibre dosage is higher. Moreover, at low fatigue loads (e.g., Fig. 2b), there is no significant change in the loading–unloading slope, reflecting only a minor increase in crack dimensions or damage, especially in the specimens that survive 2 million cycles, such as those with higher dosages of fibres (i.e., M40SF30 and M40SF45) subjected to a maximum fatigue load of 50% of $F_{R,1}$. This is in accordance with the findings of Carlesso et al. [21] that at very low fatigue loads, the damage caused during the cycles is minimal and does not significantly affect the post-fatigue flexural performance.

4 Evolution of fatigue damage

4.1 Variation of CMOD with fatigue loading

As mentioned earlier, the evolution of the maximum (or upper) CMOD, in each cycle, varies with the maximum fatigue load, as in Fig. 3 for M40SF45. The CMOD evolutions for all the different concretes are given in the Supplementary Material. The rate of increase in the upper CMOD with the cycles of loading reflects three stages of failure progression. The first stage is the stable increase of damage, with small changes in CMOD. The second stage corresponds to slow but gradually increasing damage, reflected by a linear CMOD–log N regime. In this stage, fibre bridging helps mitigate crack propagation and limit fatigue damage; higher the fibre content, more prolonged is this stage. The third stage occurs just before failure, where there is a sharp increase of crack opening and dramatic change in load-CMOD stiffness due to uncontrolled crack propagation. Such response was previously observed by Subramaniam et al. [32] and Gaedicke et al. [33] in their study of the fatigue fracture of plain concrete, with the difference that FRC exhibits crack stabilization in the second stage. Tawfiq et al. [34] has documented the three stages of fatigue cracking in polymer fibre reinforced concrete, with the third stage characterized by a rapid increase in deformations. In the present study, the transition from the second to third stage, marked on the plots, seems to occur at larger CMOD values when the fatigue loads are higher. This phenomenon is more significant in the concretes with lower fibre dosages (refer Supplementary Material). At higher fatigue loads, the crack opens more during the cycles, which mobilises the fibres further. Therefore, the fibres mitigate the effect of fatigue more, leading to larger $CMOD_{cr}$-values as the magnitude of the cyclic loading increases.

The faster increase in CMOD in the second stage of cracking, at higher fatigue loads, can be attributed to the greater energy imposed on the specimen within a short duration of time, which leads to more damage in the fracture process zone (FPZ) due to fibre pull-out and crack propagation; this is also in accordance with the results of Germano et al. [23], Vicente et al. [17] and González et al. [18]. Consequently, at higher fatigue loads, the critical size of the crack is reached earlier, and the specimen fails after fewer cycles. At higher fibre dosages, the crack growth in the second stage is inhibited by the more closely-spaced fibres across the crack faces, and the transition from second to third stage is delayed. It is also observed that specimens that withstand 2 million cycles of loading only undergo the first two stages of damage, and consequently, the residual load-carrying capacity is unaffected.

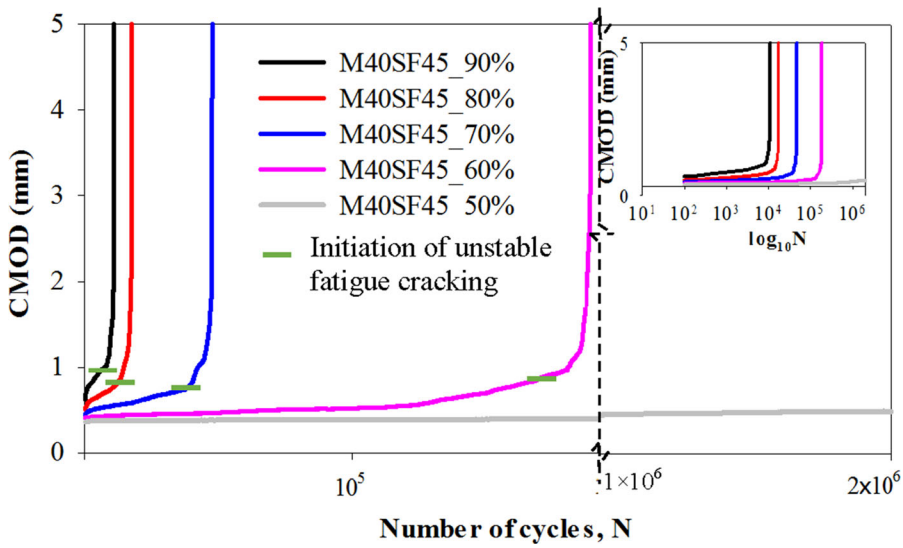

Fig. 3 Typical evolution of the upper CMOD for M40SF45 concrete (inset shows a semi-log plot)

4.2 Critical CMOD for fatigue failure

The rate of increase in the upper CMOD with cyclic loading has been computed as dCMOD/dN = ($CMOD_n - CMOD_m$)/($n - m$), with $CMOD_n$ and $CMOD_m$ being the maximum CMOD at the end of the nth and mth cycle, respectively. It is seen that the CMOD rate per cycle generally decreases and then increases (see typical plot in Fig. 4; plots for all the different concretes are given in the Supplementary Material), similar to the observations of Subramaniam et al. [32] on plain concrete. There is always a distinctive critical point, denoted here as $CMOD_{cr}$, when the transition from the second to third stage of cracking occurs, beyond which the CMOD rate starts increasing, more steeply so for specimens subjected to high fatigue loads. Further, as mentioned earlier, the $CMOD_{cr}$ increases with an increase in the fatigue load, implicating the higher cumulative energy for the failure, as proposed by Germano et al. [23]. For specimens subjected to relatively lower fatigue loads, the relaxation of stresses and the degradation of the fibre-matrix interface could lead to the reduction of residual strength and lowering of $CMOD_{cr}$.

The degradation in load-CMOD slope was seen to be more prominent in specimens loaded at higher fatigue loads (e.g., Fig. 2a). The secant stiffness, computed between the maximum and minimum loads in each cycle, has been determined using the load-CMOD response during fatigue loading (see Fig. 5 for a typical trend; such plots for all concretes are given in the Supplementary Material). It is seen that the stiffness degradation is more rapid beyond $CMOD_{cr}$, as also noted by Banjara and Ramanjaneyulu [2], though this is mitigated by an increase in fibre dosage.

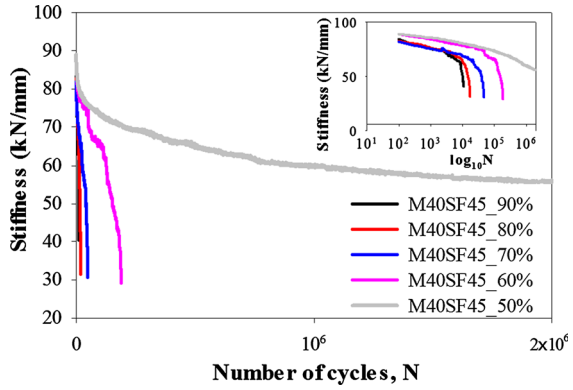

Fig. 5 Typical degradation of stiffness with fatigue cycles for M40SF45

5 Discussion of the post-peak fatigue failure process

The trend, generalised as shown in Fig. 6a, for the increase in upper CMOD during cyclic loading, is characterized by three stages of cracking (indicated in different colours in Fig. 6): the initial increase, slow stable increase and sudden unstable increase in CMOD. There is a gradual increase in CMOD with the load cycles until $CMOD_{cr}$, beyond which there is a sharp increase in CMOD prior to failure (denoted as $\times$ in Fig. 6). The corresponding increase in CMOD rate and reduction in flexural stiffness due to fatigue damage are depicted in Fig. 6b, c. During the first stage, only a small part of FPZ created earlier by the

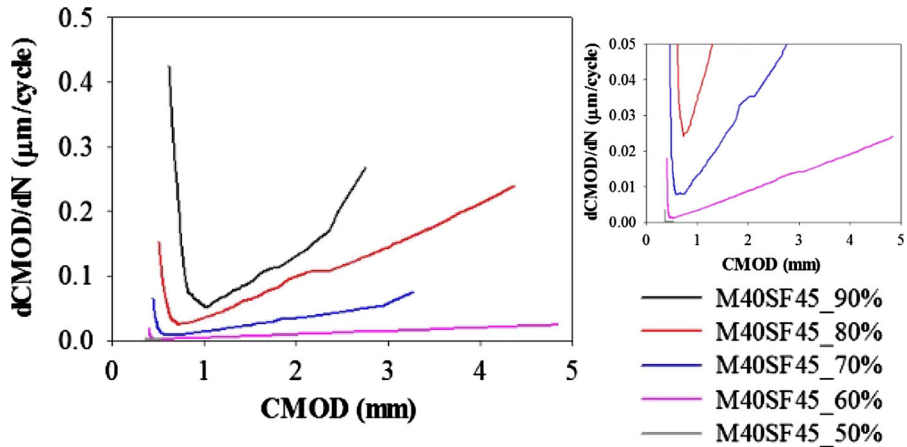

Fig. 4 Typical CMOD rate under fatigue loading for M40SF45

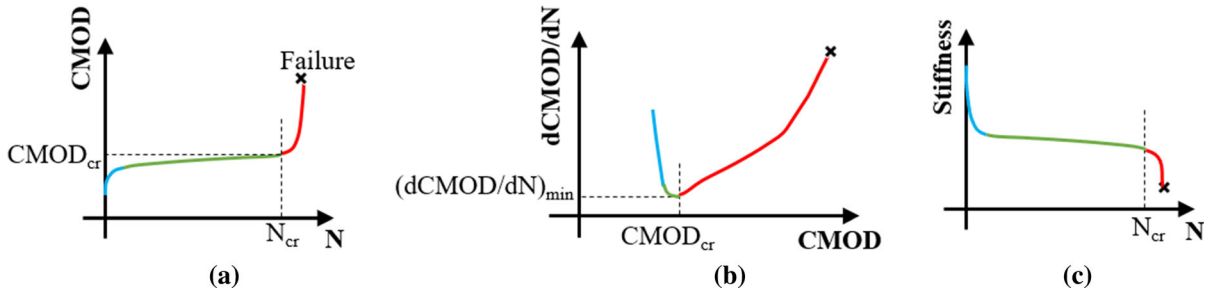

Fig. 6 Fatigue response: **a** increase in CMOD during fatigue loading, **b** rate of increase in CMOD during fatigue loading, and **c** corresponding decrease in stiffness

pre-cracking loading is under stress and only few fibres are active, during the fatigue loading. Consequently, there is an increase in CMOD but with a decreasing rate, as more fibres are activated. In the second stage, there is an increase in FPZ, with more fibres active in bridging the crack, and hence the CMOD increase is gradual or at a constant rate. After further cycles, in the third stage, the fibres break or pull out, leading to an increase in the crack length and reduction in the residual strength. This causes a rapid increase in CMOD and significant reduction in stiffness, eventually causing failure.

Based on the observations made earlier, the evolution of the FPZ in FRC during different stages of fatigue loading is hypothesised in Fig. 7, for a case of crack initiation under monotonic loading followed by propagation under cyclic loading at lower loads (see load-CMOD response in Fig. 7a). The defect or notch (of length a_0) from where the crack initiates and the material microstructure ahead of it are depicted in the Sketch A (in Fig. 7b). When load is applied, beyond the elastic limit, until a crack of small width (say, a CMOD of 0.5 mm), the FPZ can be taken to have developed over a length Δa_1, and the crack would have a length of $(a_0 + \Delta a_1)$, as in the Sketch B. The main characteristics of the FPZ would be microcracking and fibre pull-out. Upon the removal of the load, the crack closes partially and the CMOD reduces; however, the damage suffered by the concrete within the FPZ remains (i.e., over $a_0 + \Delta a_1$), as in Sketch C. When the section is subsequently subjected to cyclic loading, and the loads are much smaller than that which caused the FPZ formation, the crack opens and closes but does not propagate further until the fibre-matrix bond degrades and the bridging action is lost, leading to slow crack widening, with no significant change in stiffness, until the critical crack opening is reached (Sketch D). Beyond this, there is considerable loss in the bridging strength due to fatigue and the crack propagates further (Sketch E). This stage would occur over only few cycles, if the crack propagation $(a_0 + \Delta a_1 + \Delta a_2)$ is rapid, say due to higher loads. Also, for concrete with higher fibre dosages, more fibres resist the opening and the propagation of the FPZ is restricted.

6 *S–N* models based on the fatigue response

With the purpose of representing the effect of the fibre dosage on the fatigue response and providing parameters for structural design, *S–N* or Wöhler curves are plotted showing the maximum nominal stress applied and the corresponding number of cycles to failure. The stress applied is given as a percentage of the residual strength at a CMOD of 0.5 mm, $f_{R,1}$, calculated as per EN 14651 [30]. The semi-logarithmic plots in Fig. 8 consider data from 6 specimens at each loading level analyzed statistically based on ASTM E739-10 [35]. The generalized model is given as:

$$\log_{10} N_f = A + B \log_{10}(\%f_{R,1}) \quad (1)$$

where A and B are fatigue coefficients for each dosage, and N_f is the number cycles to failure. The experimental data and the fitted models for each concrete, along the 95% confidence intervals, are given in the Supplementary Material. The parameters obtained for each concrete are provided in Fig. 8.

When the *S–N* models for concrete without and with fibres are compared (i.e., M40SF0 and M40SF10), there is a significant shift in the regression line to the right, representing the increase in fatigue

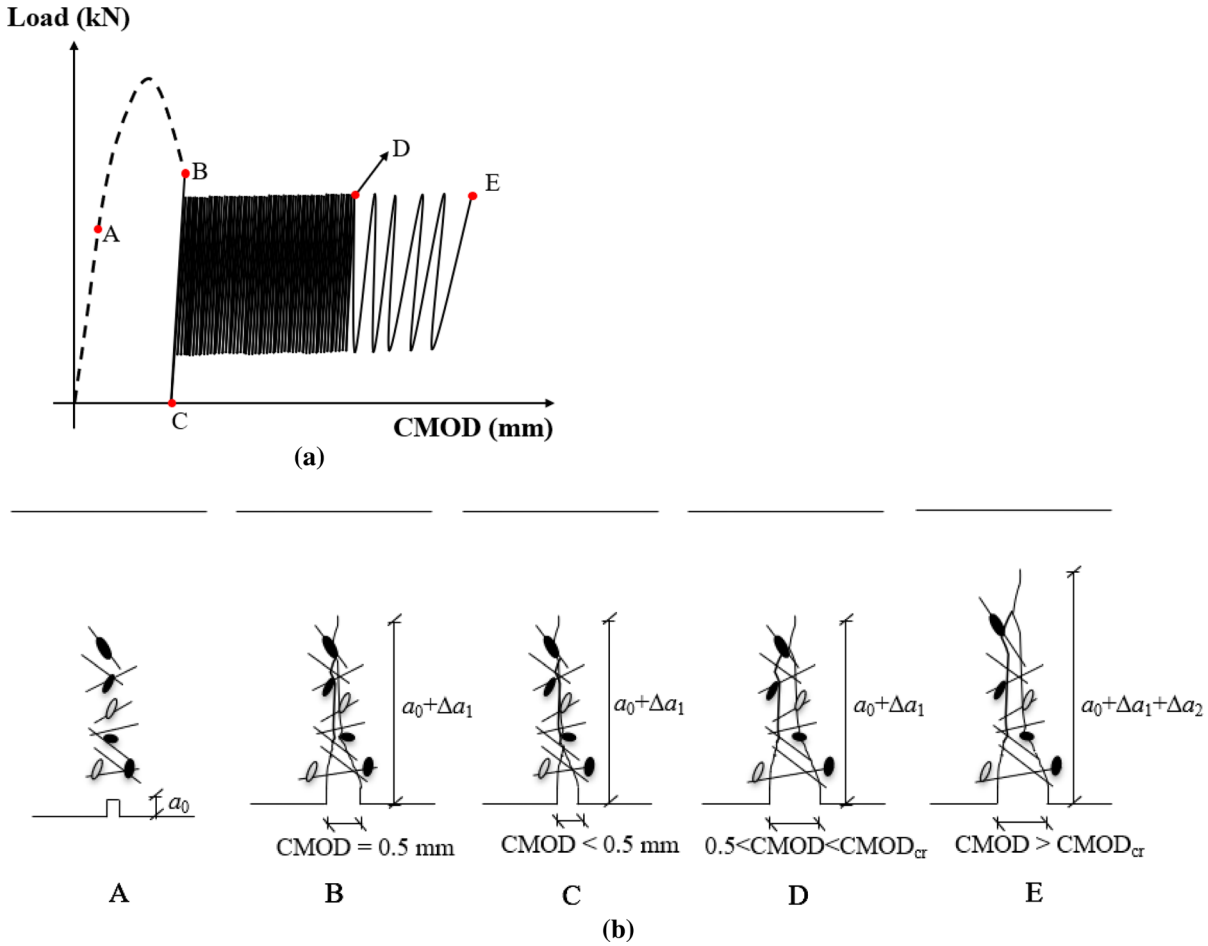

Fig. 7 **a** Typical load-CMOD response and **b** hypothesized evolution of the FPZ under cyclic loading

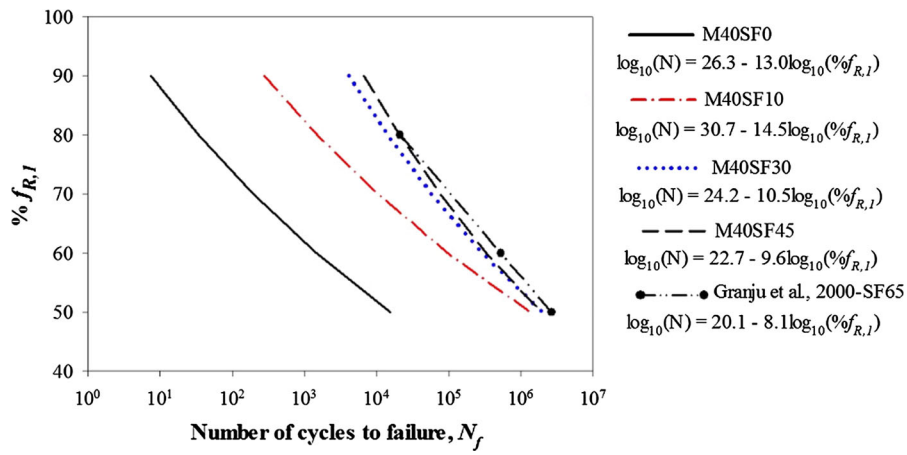

Fig. 8 Comparison of *S*–*N* models for concretes with different dosages of steel fibres

life, at all loading levels. It is conjectured that the incorporation of even a low dosage of fibres significantly improves the fatigue performance of concrete due to crack bridging and mitigation of fracture propagation. With further increase in fibre dosage, the slope of the regression line becomes steeper. This

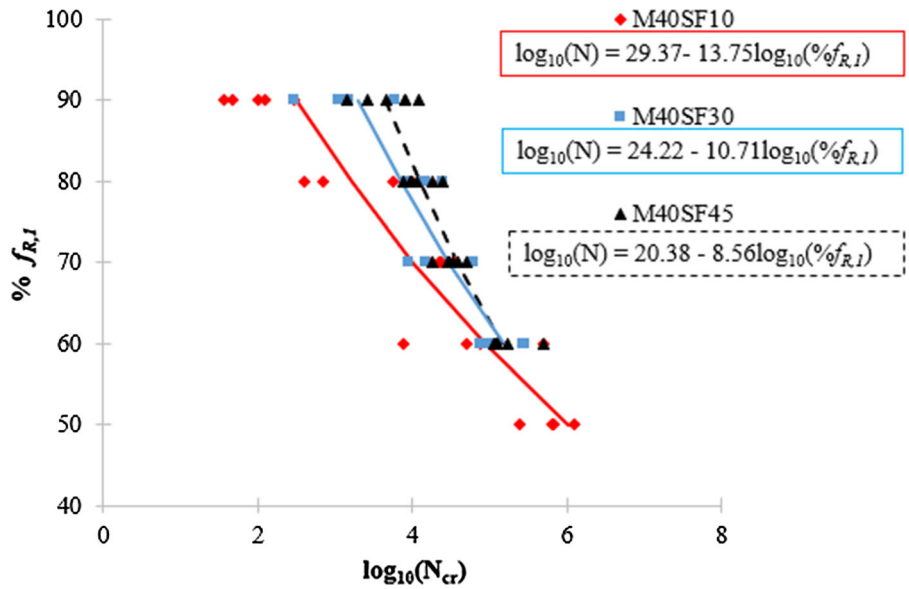

Fig. 9 *S–N* models based on critical CMOD for FRC with different dosages of steel fibres

implies that the benefit of the addition of fibre is more pronounced at higher fatigue loading levels and is not as significant at low loading levels. The fatigue lives of M40SF30 and M40SF45 are in the same of order of magnitude, which seems to imply that beyond a certain dosage the benefit of incorporating fibres for improving the fatigue life diminishes progressively. This is in line with the data of Granju et al. [26], where SFRC with 65 kg/m^3 of steel fibres was seen to have fatigue lives in the same order of magnitude as those of 45 kg/m^3; for comparison; the fit of their data is plotted along with those of the present experimental results in Fig. 8, supporting the above argument well. It can also be suggested that the probability of fatigue failure would be small when the cyclic loads are less than about 50% of the pre-cracking load (i.e., equivalent flexural stresses during the cycles are less than 50% of $f_{R,1}$), which may be considered as the endurance limit, if needed. It also appears the endurance limit in the post-peak regime is significantly lower than the limit of about 65% observed previously in the pre-peak regime [26].

The *S–N* curves given in Fig. 8 estimate the fatigue life (in terms of the number of loading cycles to failure) for different stress ratios. However, in the design of FRC structures, it may be more appropriate [34], and certainly more conservative, to consider the fatigue life in terms of the number of cycles to reach the critical crack opening, beyond which there is rapid crack widening and propagation. Accordingly, *S–N* models based on the number of cycles (N_{cr}) to reach the critical CMOD are presented in Fig. 9 for different dosages of steel fibres. The slope of these fits has a trend similar to that seen in Fig. 8, with diminishing increase in slope with an increase in the fibre dosage. These curves are proposed to be more appropriate in ultimate limit state design, especially when the crack widths are to be limited.

7 Conclusions

In this paper, the flexural fatigue performance of concrete reinforced with different dosages of hooked-ended steel fibres has been assessed. The evolution of fracture process zone with cyclic loading is studied based on the progressive increase in crack opening and degradation of stiffness. The major findings are as follows:

- The crack mouth opening displacement (CMOD) increases and the slope of the load-CMOD response decreases as the load is cycled, with a rapid change occurring when the response approaches the envelope of the monotonic curve, culminating in failure; at lower loads, the change is slower with failure occurring only after large crack

widths. Three stages of failure progression can be identified: the first stage is the stable increase of damage, with small change in CMOD; the second stage corresponds to slow but gradually increasing damage, reflected by a linear CMOD–log N regime; and the third stage is characterized by dramatic increase of crack opening and decrease in load-CMOD stiffness due to uncontrolled crack propagation.

- In the second stage, fibre bridging helps mitigate crack propagation and limit fatigue damage; higher the fibre content, more prolonged is this stage. At high fatigue loads, the bridging degrades leading to a decrease in residual load carrying capacity, eventually causing failure.
- It is seen that the CMOD rate per cycle generally decreases and then increases, with a critical point, denoted here as $CMOD_{cr}$, when the transition from the second to third stage of cracking occurs. The $CMOD_{cr}$-values are larger at higher fatigue loads due to the greater cumulative energy supplied over a short duration of time. At lower fatigue loads, the low $CMOD_{cr}$ is attributed to the relaxation of stresses and the reduction of residual strength due to the degradation of the fibre-matrix interface. The occurrence and the implications of the $CMOD_{cr}$ have been related to the development of the fracture process zone.
- In addition to the conventional *S–N* curves that define the life until unstable failure, regression analysis was carried out to develop *S–N* models corresponding to $CMOD_{cr}$. Such models could be more appropriate in ultimate limit state design, especially when crack width is to be limited.
- From the *S–N* models, it can be inferred that the incorporation of even a low dosage of fibres significantly improves the fatigue performance of concrete due to crack bridging and mitigation of fracture propagation. With further increase in dosage, the benefit of fibre addition is only significant at higher fatigue loading levels, and not pronounced at low loading levels.

Acknowledgements The authors thank M/s. Bekaert for providing the fibres used in this work. The first author is thankful to the Ministry of Human Resource Development (MHRD), Government of India, for providing an assistantship during her doctoral studies. The DST FIST Grant SR/FST/ETII-054/2012 is acknowledged for tests performed in the Laboratory for Mechanical Performance of Civil Engineering Materials, IIT Madras.

Compliance with ethical standards

Conflict of interest The authors declare that there is no conflict of interest in this work.

References

1. Gopalaratnam VS, Cherian T (2002) Fatigue characteristics of fiber reinforced concrete for pavement applications. ACI Spec Publ 206:91–108
2. Banjara NK, Ramanjaneyulu K (2018) Experimental investigations and numerical simulations on the flexural fatigue behavior of plain and fiber-reinforced concrete. J Mater Civ Eng 30:1–15. https://doi.org/10.1061/(ASCE)MT.1943-5533.0002351
3. Batson BG, Ball C, Bailey L, Landers E, Hooks J (1972) Flexural fatigue strength of steel fiber reinforced concrete beams. ACI J 69:673–677
4. Kaur G, Singh SP, Kaushik SK (2016) Influence of mineral additions on flexural fatigue performance of steel fibre reinforced concrete. Mater Struct 49:4101–4111. https://doi.org/10.1617/s11527-015-0775-3
5. Plizzari GA, Cangiano S, Alleruzzo S (1997) The fatigue behaviour of cracked concrete. Fatigue Fract Eng Mater Struct 20:1195–1206. https://doi.org/10.1111/j.1460-2695.1997.tb00323.x
6. Cangiano S, Plizzari GA, Slowik V (1998) Experimental investigation into the fatigue crack growth in concrete. In: Fracture mechanics of concrete structures proceedings FRAMCOS-3. AEDIFICATIO Publishers, Freiburg, pp 645–654
7. Müller S, Mechtcherine V (2017) Fatigue behaviour of strain-hardening cement-based composites (SHCC). Cem Concr Res 92:75–83. https://doi.org/10.1016/j.cemconres.2016.11.003
8. Schäfer N, Gudžulić V, Timothy JJ, Breitenbücher R, Meschke G (2019) Fatigue behavior of HPC and FRC under cyclic tensile loading: experiments and modeling. Struct Concr 20:1265–1278. https://doi.org/10.1002/suco.201900056
9. Cachim PB (1999) Experimental and numerical analysis of the behaviour of structural concrete under fatigue loading with applications to concrete pavements, Ph.D. thesis. University of Porto, Portugal
10. Lee MK, Barr BIG (2004) An overview of the fatigue behaviour of plain and fibre reinforced concrete. Cem Concr Compos 26:299–305. https://doi.org/10.1016/S0958-9465(02)00139-7
11. IRC:58 (2010) Guidelines for the design of plain jointed rigid pavements for highways. Indian Road Congress, New Delhi
12. IRC:SP:46 (2013) Guidelines for design and construction of fibre reinforced concrete pavements. Indian Road Congress, New Delhi

13. Naaman AE, Hammoud H (1998) Fatigue characteristics of high performance fiber-reinforced concrete. Cem Concr Compos 20:353–363. https://doi.org/10.1016/S0958-9465(98)00004-3
14. Spadea G, Bencardino F (1997) Behavior of fiber-reinforced concrete beams under cyclic loading. J Struct Eng 123:660–668
15. Chang D-I, Chai W-K (1995) Flexural fracture and fatigue behavior of steel-fiber-reinforced concrete structures. Nucl Eng Des 156:201–207
16. Johnston CD, Zemp RW (1991) Flexural fatigue performance of steel fiber reinforced concrete-influence of fiber content, aspect ratio, and type. ACI Mater J 88:374–383
17. Vicente MA, Mínguez J, González DC (2019) Computed tomography scanning of the internal microstructure, crack mechanisms, and structural behavior of fiber-reinforced concrete under static and cyclic bending tests. Int J Fatigue 121:9–19. https://doi.org/10.1016/j.ijfatigue.2018.11.023
18. González DC, Moradillo R, Mínguez J, Martínez JA, Vicente MA (2018) Postcracking residual strengths of fiber-reinforced high-performance concrete after cyclic loading. Struct Concr 19:340–351. https://doi.org/10.1002/suco.201600102
19. Ramakrishnan V, Wu GY, Hosalli G (1989) Flexural fatigue strength, endurance limit, and impact strength of fiber reinforced concretes. Transp Res Rec J Transp Res Board 1226:17–24
20. Zhang J, Stang H, Li VC (1999) Fatigue life prediction of fibre reinforced concrete under flexural load. Int J Fatigue 21:1033–1049. https://doi.org/10.1016/S0142-1123(99)00093-6
21. Carlesso DM, de la Fuente A, Cavalaro SHP (2019) Fatigue of cracked high performance fiber reinforced concrete subjected to bending. Constr Build Mater 220:444–455. https://doi.org/10.1016/j.conbuildmat.2019.06.038
22. Nayar SK (2015) Design of fibre reinforced concrete slabs-on-grade and pavements. PhD thesis. Indian Institute of Technology Madras, India
23. Germano F, Tiberti G, Plizzari G (2015) Post-peak fatigue performance of steel fiber reinforced concrete under flexure. Mater Struct 49:4229–4245. https://doi.org/10.1617/s11527-015-0783-3
24. ACI 544.7R (2016) Report on design and construction of fiber-reinforced precast concrete tunnel segments. American Concrete Institute, Farmington Hills
25. TR34 (2003) Concrete industrial ground floors, a guide to design and construction. The Concrete Society, UK
26. Granju J, Rossi P, Chanvillard G, Mesureur B, Turatsinze A, Farhat H, Boulay C, Serrano J-J, Fakhri P, Roque O, Rivillion P (2000) Delayed behaviour of cracked SFRC beams. In: Fifth RILEM symposium on fibre-reinforced concrete, pp 511–520
27. Murdock JW (1965) A critical review of research on fatique of plain concrete. Engineering Experiment Station. Bulletin 475. College of Engineering, University of Illinois at Urbana Champaign, USA
28. Lloyd JP, Loft JL, Kesler CE (1968) Fatigue of concrete. University of Illinois at Urbana Champaign, College of Engineering. Engineering Experiment Station, Urbana
29. Shukla SP, Yadav SK, Lohani B, Behera SN (2012) Characterization of traffic noise for a typical Indian road crossing Characterization of traffic noise for a typical Indian road crossing. Curr Sci 103:1193–1201
30. EN 14651 (2005) Test method for metallic fibre concrete-Measuring the flexural tensile strength (limit of proportionality (LOP), residual). European Standards, Brussels
31. Stephen SJ, Gettu R (2019) Rate-dependence of the tensile behaviour of fibre reinforced concrete in the quasi-static regime. Mater Struct 52:107. https://doi.org/10.1617/s11527-019-1405-2
32. Subramaniam KV, O'Neil E, Popovics JS, Shah SP (2000) Crack propagation in flexural fatigue of concrete. J Eng Mech 126:891–898
33. Gaedicke C, Roesler J, Shah S (2009) Fatigue crack growth prediction in concrete slabs. Int J Fatigue 31:1309–1317. https://doi.org/10.1016/j.ijfatigue.2009.02.040
34. Tawfiq K, Armaghani J, Ruiz R (1999) Fatigue cracking of polypropylene fiber reinforced concrete. ACI Mater J 96:226–233. https://doi.org/10.14359/449
35. ASTM E739-10 (2015) Standard practice for statistical analysis of linear or linearized stress-life (S-N) and strain-life (ε-N) fatigue data. American Standard for Testing of Materials, USA